CHEMISTRY
A EUROPEAN JOURNAL

DOI: 10.1002/chem.200601846

Hydrolysis of Dinuclear Ruthenium Complexes $[\{CpRu(PPh_3)_2\}_2(\mu,\eta^{1:1}\text{-}L)][CF_3SO_3]_2$ ($L = P_4, P_4S_3$): Simple Access to Metal Complexes of P_2H_4 and PH_2SH

Pierluigi Barbaro,[b] Massimo Di Vaira,[a] Maurizio Peruzzini,[b] Stefano Seniori Costantini,[a] and Piero Stoppioni*[a]

Abstract: The reaction of $[CpRu(PPh_3)_2Cl]$ (**1**) with half an equivalent of P_4 or P_4S_3 in the presence of $AgCF_3SO_3$ as chloride scavenger affords the stable dimetal complexes $[\{CpRu(PPh_3)_2\}_2(\mu,\eta^{1:1}\text{-}P_4)][CF_3SO_3]_2\cdot 3\,CH_2Cl_2$ (**2**) and $[\{CpRu(PPh_3)_2\}_2(\mu,\eta^{1:1}\text{-}P_{apical}\text{-}P_{basal}\text{-}P_4S_3)][CF_3SO_3]_2\cdot 0.5\,C_7H_8$ (**3**), in which the tetrahedral P_4 and mixed-cage P_4S_3 molecules are respectively bound to two $CpRu(PPh_3)_2$ fragments through two phosphorus atoms. The coordinated cage molecules, at variance with the free ligands, readily react with an excess of water in THF under mild conditions. Among the hydrolysis products, the new, remarkably stable complexes $[\{CpRu(PPh_3)_2\}_2(\mu,\eta^{1:1}\text{-}P_2H_4)][CF_3SO_3]_2$ (**4**) and $[CpRu(PPh_3)_2(\eta^1\text{-}PH_2SH)]CF_3SO_3$ (**8**) were isolated. In the former, diphosphane, P_2H_4, is coordinated to two $CpRu(PPh_3)_2$ fragments, and in the latter thiophosphinous acid, H_2PSH, is coordinated to the metal centre through the phosphorus atom. All compounds were characterised by elemental analyses and IR and NMR spectroscopy. The crystal structures of **2**, **3**, **4** and **8** were determined by X-ray diffraction.

Keywords: hydrolysis · P ligands · phosphane ligands · phosphorus · ruthenium

Introduction

In recent years the chemistry of white phosphorus P_4 and tetraphosphorus trisulfide P_4S_3 in the presence of transition-metal fragments has been widely investigated.[1–9] Many compounds containing P_x or P_xS_y units originating from degradation of the parent molecules or reaggregation of fragments thereof have been synthesised and characterised. These compounds, besides having unique geometric and electronic properties,[10] have also proved useful for obtaining networks of inorganic coordination compounds,[11] including polymeric 1D and 2D structures,[12] and inorganic fullerene-like molecules.[13] These studies usually involved reactions of P_4 and P_4S_3 with metal moieties under harsh conditions. Indeed, the number of coordination complexes featuring the intact cagelike molecules as ligands are limited to very few examples, which are usually thermally unstable and/or difficult to handle.[14–21] Accordingly, the reactivity of the coordinated molecules has not been investigated. Recently, 16-electron rhenium,[22] iron[23] and ruthenium[23] moieties have been found to coordinate the intact P_4 and P_4S_3 molecules and to form stable and soluble compounds in gram amounts. Therefore, these complexes are suitable as starting materials for investigating the reactivity of the coordinated molecules. As recently highlighted also by Cummins et al. in a study on the activation of white phosphorus by molybdenum complexes,[24] this topic is of particular interest in view of the attractive possibility to obtain organophosphorus and/or organosulfur compounds by mild activation of the coordinated intact molecules. Recently, we found that the P_4 unit in $[CpRu(PPh_3)_2(\eta^1\text{-}P_4)]Y$ ($Y = PF_6$, CF_3SO_3) readily undergoes disproportionation with water under mild conditions.[25] Fine-tuning the properties of the metal fragment plays an important role in determining the outcome of the reaction. For example, $[Cp^*Ru(PPh_3)_2(\eta^1\text{-}P_4)]Y$ ($Cp^* =$ pentamethylcyclopentadienyl) complexes do not undergo hydrolysis under the same conditions.[23] The products obtained from the hydrolysis of $[CpRu(PPh_3)_2(\eta^1\text{-}P_4)]Y$ are

---

[a] Prof. Dr. M. Di Vaira, Dr. S. Seniori Costantini, Prof. Dr. P. Stoppioni
Dipartimento di Chimica, Università di Firenze
via della Lastruccia, 3, 50019 Sesto Fiorentino, Firenze (Italy)
Fax: (+39) 055-457-3385
E-mail: piero.stoppioni@unifi.it

[b] Dr. P. Barbaro, Dr. M. Peruzzini
ICCOM CNR, via Madonna del Piano, 10
50019 Sesto Fiorentino, Firenze (Italy)

Supporting information for this article is available on the WWW under http://www.chemeurj.org/ or from the author.

phosphine, which remains coordinated to the metal to yield the complex [CpRu(PPh_3)$_2$(PH_3)]Y, and a number of oxygenated phosphorus compounds, among which phosphorous and hypophosphorous acids were identified.[25]

In the presence of the [(triphos)Re^{I}(CO)$_2$] (triphos = 1,1,1-tris(diphenylphosphanyl)methane)[22,26] and [Cp*Ru^{II}(L_2)][27] (L_2 = diphosphane) fragments both P_4 and P_4S_3 form dinuclear complexes, characterised only in solution, in which the cage molecule tethers two metal moieties through two phosphorus atoms. Finally, the moisture- and air-sensitive homoleptic P_4S_3 silver complex [Ag(P_4S_3)$_2$][Al(pftb)$_4$] (pftb = OC(CF_3)$_3$), recently described by Krossing et al., forms a one-dimensional polymeric chain with P,S coordination of the cage.[28]

In view of the ability of the CpRu(PPh_3)$_2$ fragment to coordinate and activate the P_4 molecule, we synthesised dinuclear complexes with bridging P_4 or P_4S_3 ligands with the aim of studying their reactivity in comparison with the mononuclear species. Here we report the synthesis of the highly stable dimetal complexes [{CpRu(PPh_3)$_2$}$_2$($\mu,\eta^{1:1}$-P_4)][CF_3SO_3]$_2$·3CH_2Cl_2 (**2**) and [{CpRu(PPh_3)$_2$}$_2$($\mu,\eta^{1:1}$-P_{apical}-P_{basal}-P_4S_3)][CF_3SO_3]$_2$·0.5C_7H_8 (**3**). In THF at room temperature, these complexes readily react with an excess of water to yield several products, most of which were isolated and characterised. They include [{CpRu(PPh_3)$_2$}$_2$($\mu,\eta^{1:1}$-P_2H_4)][CF_3SO_3]$_2$ (**4**) and [CpRu(PPh_3)$_2$(η^1-PH_2SH)]CF_3SO_3 (**8**). In the former, diphosphane P_2H_4 bridges two CpRu(PPh_3)$_2$ units, while the latter contains the practically unknown thiophosphinous acid H_2PSH, bound to the metal centre through the phosphorus atom. All the new complexes were fully characterised by elemental analyses and IR and NMR measurements. The crystal structures of **2**, **3**, **4** and **8** were determined by X-ray diffraction.

Results and Discussion

The reaction of [CpRu(PPh_3)$_2$Cl] (**1**) in THF/CH_2Cl_2 with half an equivalent of P_4 or P_4S_3 in the presence of $AgCF_3SO_3$ as chloride scavenger leads to precipitation of AgCl and formation of the complexes [{CpRu(PPh_3)$_2$}$_2$($\mu,\eta^{1:1}$-P_4)][CF_3SO_3]$_2$·3CH_2Cl_2 (**2**) or [{CpRu(PPh_3)$_2$}$_2$($\mu,\eta^{1:1}$-P_{apical}-P_{basal}-P_4S_3)][CF_3SO_3]$_2$·0.5C_7H_8 (**3**) as orange or yellow microcrystals, respectively, in good yield (Scheme 1). The P_4 complex **2** is also obtained by adding a stoichiometric amount of the CpRu(PPh_3)$_2$ moiety, generated in situ from **1**, to [CpRu(PPh_3)$_2$(η^1-P_4)]CF_3SO_3.[25] Compounds **2** and **3** are stable under inert atmosphere and are soluble in common organic solvents. Although we recently described some rhenium and ruthenium complexes containing intact P_4[26,27] or P_4S_3[22] units bridging two metal centres, no crystal structure of these complexes has been reported to date.

The X-ray structures of the cations in compounds **2** and **3** are shown in Figures 1 and 2, respectively, and selected geometrical parameters are listed in Tables 1 and 2.

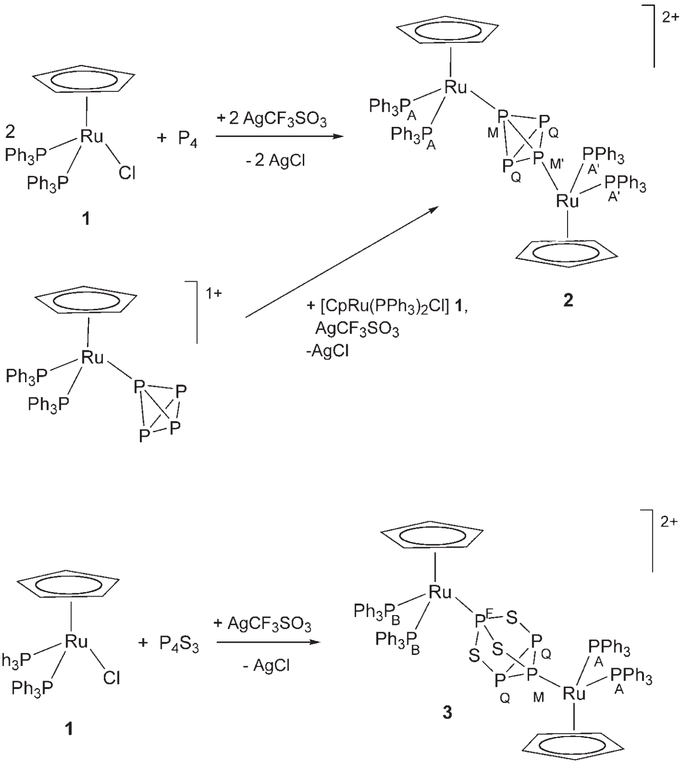

Scheme 1.

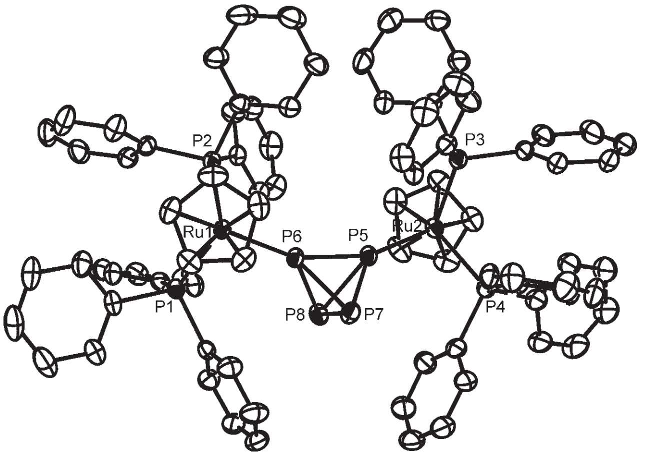

Figure 1. A view of the cation in the structure of **2**, with 30 % probability ellipsoids. Hydrogen atoms are omitted for clarity.

The dimetal cation in **2**, which crystallises as a dichloromethane solvate, has idealised twofold rotational symmetry around an axis bisecting two opposite P–P edges of the tetrahedral P_4 cage, which is rather tightly shielded by the phosphane and Cp ligands. The coordination geometry of the metal atoms does not differ considerably from that in the monometal cation [CpRu(PPh_3)$_2$(η^1-P_4)]$^+$,[25] the main differences consisting of a wider spread of the P(PPh_3)-Ru-P(P_4) angles (9.9 vs. 4.6°) and slightly longer Ru–P(P_4) distances (by 0.022 Å on average) in **2** than in the monometal complex. The P_4 cage in **2** exhibits small distortions from

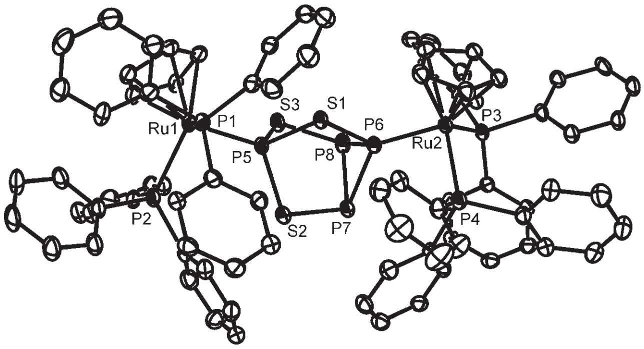

Figure 2. A view of the cation in the structure of **3**, with 30 % probability ellipsoids. Hydrogen atoms are omitted for clarity.

Table 1. Selected bond lengths [Å] and angles [°] for **2**.

Ru1–P1	2.369(1)	Ru2–P3	2.350(1)
Ru1–P2	2.340(1)	Ru2–P4	2.370(2)
Ru1–P6	2.286(1)	Ru2–P5	2.297(1)
P5–P6	2.161(2)	P5–P7	2.195(2)
P6–P7	2.180(2)	P5–P8	2.180(2)
P6–P8	2.189(2)	P7–P8	2.215(2)
P1-Ru1-P2	99.48(5)	P3-Ru2-P4	99.58(5)
P1-Ru1-P6	91.50(5)	P3-Ru2-P5	101.27(5)
P2-Ru1-P6	97.67(5)	P4-Ru2-P5	91.68(5)
Ru1-P6-P5	159.12(8)	Ru2-P5-P6	160.38(8)

Table 2. Selected bond lengths [Å] and angles [°] for **3**.

Ru1–P1	2.353(2)	Ru2–P3	2.349(2)
Ru1–P2	2.393(2)	Ru2–P4	2.363(2)
Ru1–P5	2.254(2)	Ru2–P6	2.279(2)
P5–S1	2.113(2)	P8–S3	2.073(2)
P5–S2	2.125(2)	P6–P7	2.214(2)
P5–S3	2.122(2)	P6–P8	2.248(2)
P6–S1	2.089(2)	P7–P8	2.276(2)
P7–S2	2.076(2)		
P1-Ru1-P2	101.22(5)	P3-Ru2-P4	101.24(5)
P1-Ru1-P5	95.75(6)	P3-Ru2-P6	95.96(5)
P2-Ru1-P5	96.52(5)	P4-Ru2-P6	92.65(5)

regular tetrahedral geometry, in that the P–P bond formed by the coordinating phosphorus atoms is 0.054 Å shorter than the opposite P–P bond, which in turn is 0.029 Å longer than the other four P–P bonds of the cage (av 2.186(7) Å). The mean of the six P–P distances in **2** is 0.02 Å larger than the corresponding mean for the monometal P_4 complex.[25] Since a geometry optimisation performed by quantum mechanical calculations on a gas-phase model yielded the same type of cage deformation as found experimentally, it should be ascribed to electronic effects rather than to the effect of packing forces in the solid (for details, see Supporting Information).

In the structure of **3**, which crystallises as a toluene solvate, the P_4S_3 cage molecule bridges the metal atoms of the two $CpRu(PPh_3)_2$ moieties through the apical P atom and one basal P atom. The $Ru–P_{apical}$ distance is slightly shorter than the $Ru–P_{basal}$ one, and both are shorter than the $Ru–P(P_4)$ distances in **2** (Table 1 and Table 2). The P_4S_3 cage exhibits small distortions from regularity: the two P–S bonds formed by the sulfur atom bound to the coordinating phosphorus atoms are slightly shorter ($P_{apical}–S$) and slightly longer ($P_{basal}–S$), respectively, than the other P–S bonds of corresponding type in the cage. In addition, the P–P bond between non-coordinating phosphorus atoms is slightly longer than the other two basal P–P bonds. Again, this trend is substantially matched by the geometry of a computationally optimised model (Supporting Information), so it should not be ascribed to packing effects in the solid. The same mode of coordination by the P_4S_3 molecule, through the apical and a basal P atom, has been found for the smaller fraction in the disordered structure of a silver complex;[28] however, effects of disorder and differences both in the nature of the metals involved and in their environments, prevent detailed comparisons between this structure and that of **3**.

The $^{31}P\{^1H\}$ NMR spectra of **2** and **3** clearly show that the P_4 and the P_4S_3 molecules are firmly coordinated to both metal atoms in solution. No resonances attributable to dissociation are observed in either case in $CDCl_3$ at room temperature. Compound **2** exhibits a $^{31}P\{^1H\}$ NMR coupling pattern fully simulated as an $A_2A'_2MM'Q_2$ spin system (Figure 3), in which A and A′ are the triphenylphosphane phosphorus atoms, M and M′ are the P_4 atoms bound to the

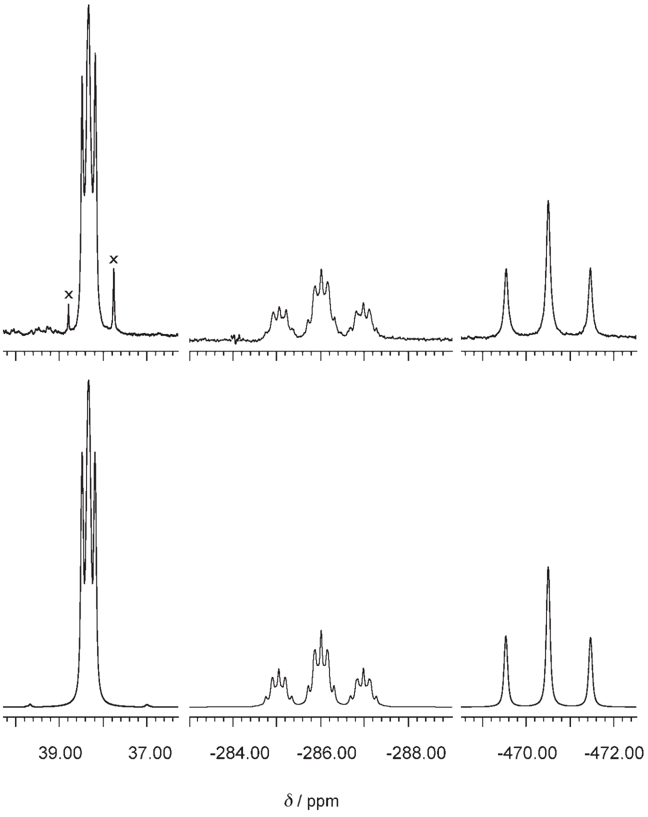

Figure 3. Computed (bottom) and experimental (top) $^{31}P\{^1H\}$ NMR spectra of **2**. Traces of impurities are marked with ×.

metal and Q the two atoms of the tetraphosphorus tetrahedron not involved in coordination (see Scheme 1 for labels). The signals of coordinated P_4 are shifted downfield with respect to the free molecule ($\Delta\delta P_{M,M'} = 239.99$, $\Delta\delta P_Q = 55.59$ ppm), and this shift is particularly enhanced for the two atoms bound to the metal centres.

Complex **3** yields a first-order $A_2B_2FMQ_2$ spin system (see Scheme 1 for labels). The triphenylphosphane P atoms (P_A and P_B) appear as two doublets due to coupling with the P_{apical} or P_{basal} atoms of the P_4S_3 cage. Both the chemical shifts and the coupling constants of the P_A and P_B nuclei show values in the range expected for cationic ruthenium half-sandwich compounds.[29] The four phosphorus atoms of the cage form the FMQ_2 part of the spectrum: the apical (P_F) and basal phosphorus atoms (P_M) exhibit two doublets of triplets of triplets due to coupling between themselves, to P_Q and to the phosphorus atoms of the triphenylphosphane ligands. All resonances are shifted downfield with respect to the free P_4S_3 molecule ($\Delta\delta P_F = 77.4$, $\Delta\delta P_M = 131.1$, $\Delta\delta P_Q = 2.2$ ppm) and, as observed for compound **2**, the phosphorus atoms bound to the metal atoms (P_M and P_F) appear to be particularly deshielded. An analogous trend has been observed for the cations $[\{(\text{triphos})Re(CO)_2\}_2(\mu,\eta^{1:1}\text{-}P_{apical}\text{-}P_{basal}\text{-}P_4S_3)]^{2+}$ and $[\{Cp^*Ru(L_2)\}_2(\mu,\eta^{1:1}\text{-}P_{apical}\text{-}P_{basal}\text{-}P_4S_3)]^{2+}$, containing a bridging P_4S_3 ligand.[22,27]

When a solution of **2** or **3** in THF was treated with an excess of water (1:100), unexpected hydrolysis of the P_4 and P_4S_3 ligands readily occurred at room temperature. Reactions carried out on different batches are reproducible, both with respect to the amount and nature of the products obtained. The $^{31}P\{^1H\}$ NMR spectrum of the solid obtained from the hydrolysis of **2** shows the presence of a mixture of several compounds, the percentages of which were estimated with respect to the four phosphorus atoms in **2** by careful integration. These compounds include free phosphorous acid (17%), the diphosphane complex cation $[\{CpRu(PPh_3)_2\}_2(\mu,\eta^{1:1}\text{-}P_2H_4)]^{2+}$ (**4**) (9%) and the known ruthenium cationic species $[CpRu(PPh_3)_2\{PH(OH)_2\}]^+$ (**5**; 9%), $[CpRu(PPh_3)_2\{P(OH)_3\}]^+$ (**6**; 6%) and $[CpRu(PPh_3)_2(PH_3)]^+$ (**7**; 9%). Further products, which defy first-order analysis and amount to about 40% of the four phosphorus atoms of starting P_4 dimetal complex **2**, are also formed, and this suggests the existence of a complicated hydrolysis pathway for the sandwiched P_4 ligand. Phosphorous acid, which was removed by extraction with water, was identified by comparison of its ^{31}P NMR spectrum with that of a pure specimen of the acid in the same solvent. Cations **5** and **6**, containing the phosphane tautomers of hypophosphorous and phosphorous acid, respectively,[30] and **7**, containing coordinated PH_3,[25] were identified by the comparison of the $^{31}P\{^1H\}$ NMR spectra with those of the pure complexes obtained by other synthetic routes recently described by us.[30] Selective precipitation from the solution of the hydrolysed compounds allowed isolation of pure **4** as a yellow powder which is soluble in common organic solvents. Recrystallisation from acetone and diethyl ether afforded crystals of **4** suitable for X-ray diffraction analysis.

The dimetal cation in the structure of **4** (Figure 4) contains an unprecedented P_2H_4 ligand that bridges two $CpRu(PPh_3)_2$ moieties in a centrosymmetric arrangement. The coordination geometry around the symmetry-independent metal atom (Table 3) is closely similar to those of **2** and **3**. The Ru–P distance formed by the bridging P_2H_4 unit is in the range of those formed by the phosphorus atoms of the cage molecules in **2** and **3** and the P–P distance of 2.211(2) Å is comparable to that of the longest P–P bond formed by the naked phosphorus atoms in the P_4 cage of **2**. To our knowledge, no structure is available for detailed comparison with **4**, as far as the P_2H_4 unit is concerned.

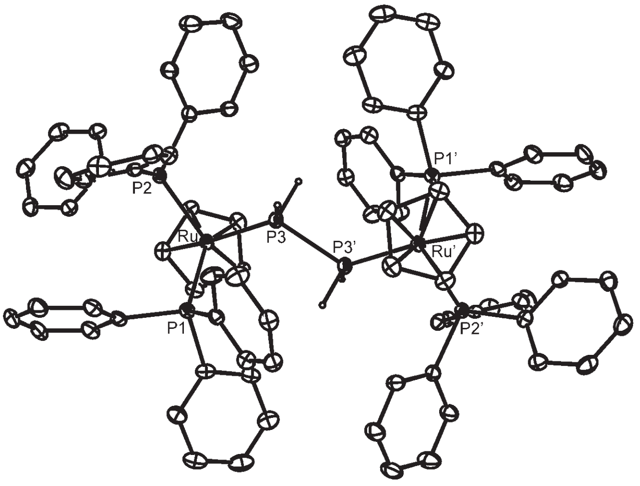

Figure 4. A view of the centrosymmetric cation in the structure of **4**, with 30% probability ellipsoids. Hydrogen atoms are omitted, except for those of the P_2H_4 bridge. Symmetry operation: ′: $1-x$, $1-y$, $-z$.

Table 3. Selected bond lengths [Å] and angles [°] for **4**.[a]

Ru–P1	2.346(1)	Ru–P3	2.280(1)
Ru–P2	2.375(1)	P3–P3′	2.211(2)
P1-Ru-P2	103.15(4)	P2-Ru-P3	91.74(4)
P1-Ru-P3	93.90(4)	Ru-P3-P3′	123.35(7)

[a] Symmetry operation: $1-x$, $1-y$, $-z$.

The $^{31}P\{^1H\}$ NMR spectrum of **4** shows a second-order $A_2A'_2MM'$ spin system, in which A and A′ are the triphenylphosphane P atoms, and M and M′ the phosphorus atoms of the two PH_2 groups. The NMR parameters were obtained through computer simulation of the experimental spectrum (Figure 5). Compound **4** is the first fully characterised complex containing a P_2H_4 ligand. Indeed, although many complexes bearing substituted diphosphanes coordinated to metal fragments have been described,[31] only a few rather unstable complexes contain P_2H_4. Among these, $[Mo(CO)_5(P_2H_4)]$,[32] poorly characterised, is rather uncertain and two others, $[\{Cr(CO)_5\}_2(P_2H_4)]$ and $[\{CpMn(CO)_2\}_2(P_2H_4)]$,[33] which contain two manganese or chromium carbonyl fragments bound to an end-on diphosphane, have been charac-

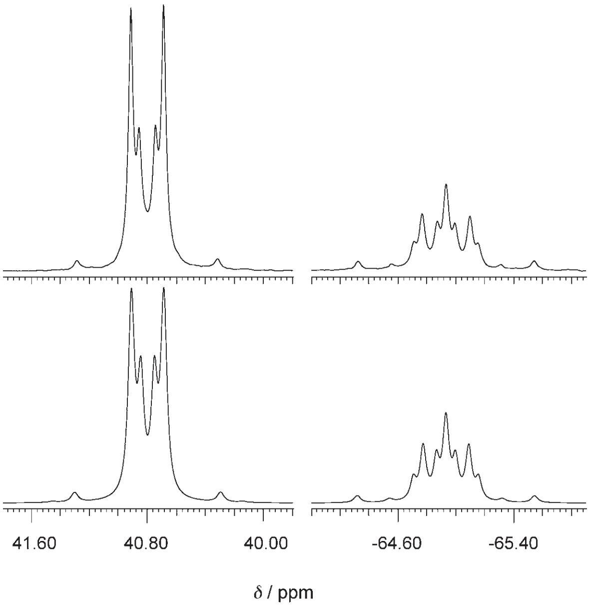

Figure 5. Computed (bottom) and experimental (top) $^{31}P\{^1H\}$ NMR spectra of **4**.

terised only by elemental analyses and spectral (IR and NMR) data. Remarkably, the diphosphane molecule, which in the free state can be handled only with special safety precautions,[34] is remarkably stabilised by coordination to two $CpRu(PPh_3)_2$ moieties.

The variety of compounds produced by disproportionation of the coordinated P_4 molecule shows that the hydrolysis, at least under the present conditions, occurs by complex pathways and makes it difficult to propose any mechanistic hypothesis. However, it is likely that $[\{CpRu(PPh_3)_2\}_2(\mu,\eta^{1:1}\text{-}P_2H_4)][CF_3SO_3]_2$ forms directly from the hydrolysis of the dimetallic tetraphosphorus complex **2**, rather than from reaggregation of intermediates with formation of transient diphosphane, as P_2H_4 decomposes at temperatures higher than −30 °C.[34] Further studies are in progress to isolate and characterise other species which are formed during the hydrolysis of the doubly coordinated P_4 molecule in **2**.

Hydrolysis of dimetal P_4S_3 complex **3** at room temperature yields H_2S and, after workup, leaves a solid residue. The ^{31}P NMR spectrum shows that the solid contains free hypophosphorous (23 %) and phosphorous acids (25 %), the cations $[CpRu(PPh_3)_2\{PH(OH)_2\}]^+$ (**5**; 2 %), $[CpRu(PPh_3)_2\{P(OH)_3\}]^+$ (**6**; 25 %) and the new complex cation $[CpRu(PPh_3)_2(\eta^1\text{-}PH_2SH)]^+$ (**8**; 25 %). The percentages of the compounds, normalised to the four phosphorus atoms of the P_4S_3 parent cage, were evaluated by careful integration of the ^{31}P signals. Remarkably, neither free nor coordinated PH_3, as in complex **7**, was detected in the hydrolysis batch. The two acids and complex cations **5** and **6** were identified by comparison of the ^{31}P NMR spectrum of the mixture with those of pure samples.[30] The new complex $[CpRu(PPh_3)_2(\eta^1\text{-}PH_2SH)]CF_3SO_3$ (**8**) was separated from the mixture by selective precipitation as a yellow solid, recrystallised and characterised by X-ray crystallography and IR and NMR spectroscopy.

The structure of the cation in the X-ray structure of **8** is shown in Figure 6 and selected bond lengths and angles are listed in Table 4. The coordination geometry around the metal centre is in close agreement with those in the dimetal derivatives reported above. The Ru−P distance formed by the H_2PSH unit is at the lower end of the 2.250–2.297 Å range of distances formed to the metal by the non-phosphane P atoms in the present compounds. The Ru-P-S angle of 122.02(5)° is close to the Ru-P-P angle of 123.35(7)° in **4**. The thiophosphinous sulfur atom is involved in a weak hydrogen-bonding interaction with an oxygen atom of the triflate anion (Table 4 and Supporting Information). To the best of our knowledge, no other structure in which the H_2PSH group is bound to a metal atom is available for comparison. In $[\{Cr(CO)_5\}_2P(Me)_2SH]$ a P−S distance of 2.019 Å and a Cr-P-S angle of 113.86 are found.[35] The formally double bonded P−S distance of 1.941(2) Å found for a tungsten PS derivative[36] is definitely shorter than the present one.

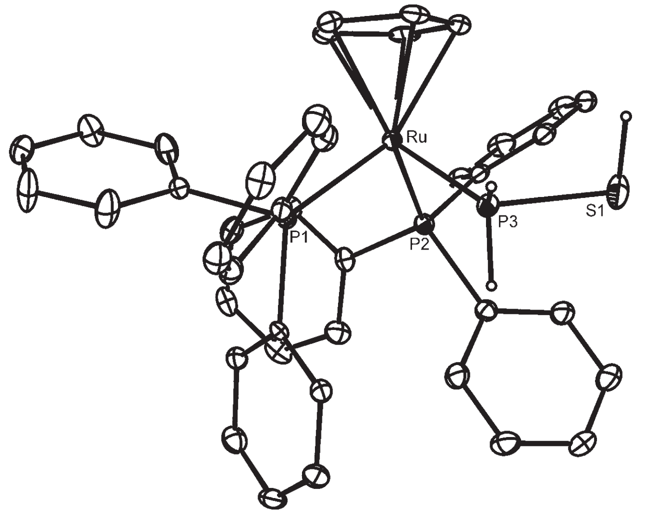

Figure 6. A view of the cation in the structure of **8**, with 30 % probability ellipsoids. Hydrogen atoms are omitted, except for those of the PH_2SH group.

Table 4. Selected bond lengths [Å] and angles [°] for **8**.

Ru−P1	2.355(1)	P3−S1	2.109(1)
Ru−P2	2.356(1)	S1−H3	1.30(4)
Ru−P3	2.250(1)	S1···O3	3.415(3)
P1-Ru-P2	101.67(3)	Ru-P3-S1	122.02(5)
P1-Ru-P3	88.33(3)	P3-S1-H3	94.8(2)
P2-Ru-P3	90.49(3)	S1-H3···O3	159(2)

The ^1H, $^1H\{^{31}P\}$ and $^{31}P\{^1H\}$ NMR spectra of **8** in $CDCl_3$, recorded over the temperature range 203–303 K, confirm that the solid-state structure of **8** is retained in solution. The $^{31}P\{^1H\}$ spectra, apart from minor changes in chemical shifts, are temperature-independent and can be attributed to an

A_2M spin system, in which A are the phosphorus atoms of the triphenylphosphane ligands and M is the phosphorus atom of thiophosphinous acid, which resonates at −32.63 ppm. On the other hand, both the ^1H and the $^1H\{^{31}P\}$ spectra in the PH_2 region are consistent with an AA′MXX′ spin system (in which A, A′ and M are the phosphorus atoms of the triphenylphosphane and PH_2SH ligands, respectively, and X, X′ are the hydrogen atoms of the PH_2 group), the pattern of which can be successfully simulated (Figure 7) only on the basis of an exchange process between P_A and $P_{A'}$ ($k_{exch}=45.6\,s^{-1}$). ^1H NOESY spectra of **8** recorded out in non-deuterated solvents do not show any exchange cross-peaks attributable to PH_2 or SH protons. The nature of the dynamic process, however, is not yet clear, although it is likely due to the presence of the acidic SH proton rather than the two PH_2 hydrogen atoms. This conclusion follows from the absence of any detectable dynamic process in the ^1H NMR spectrum of the parent complex $[CpRu(PPh_3)_2(PH_2Ph)]CF_3SO_3$ (**9**) in which PH_2SH has been replaced with PH_2Ph. This complex, which is readily synthesised by reaction of **1** and PH_2Ph in the presence of silver triflate in THF/CH_2Cl_2, gives NMR data in agreement with the proposed formula and similar to those found for **8**. The stability of **8**, the first complex containing the H_2PSH molecule, is quite remarkable in view of the extreme instability of the free compound, which was generated only at very low temperature by glow discharge in a mixture of H_2S and PH_3[37] or trapped in solid argon matrices after discharge in PH_3/S_8 mixtures.[38] The crystal structure of the complex provides important information on the H_2PSH molecule, which, although never prepared in a chemical laboratory, has been widely considered in theoretical work due to its relevance to an understanding of the behaviour of aliphatically and aromatically substituted phosphine sulfides.[39]

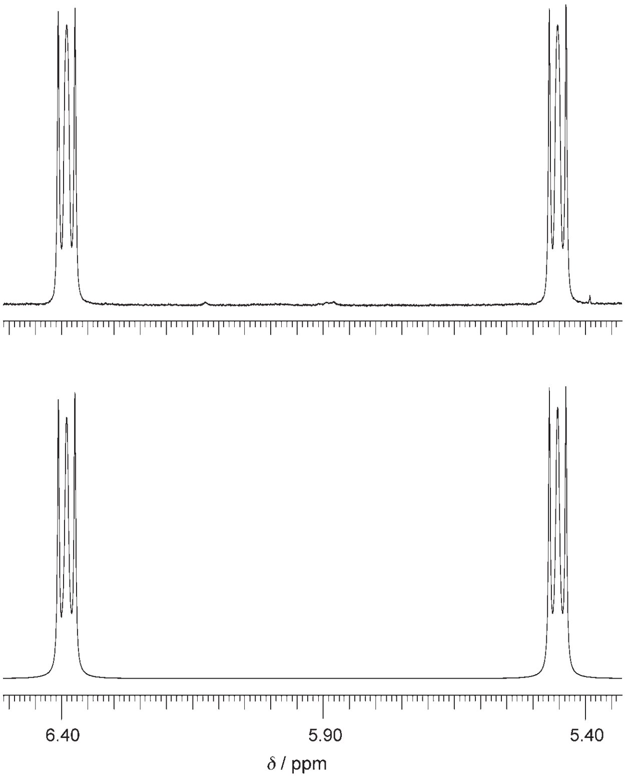

Figure 7. Section of the computed (bottom) and experimental (top) ^1H NMR spectra of **8** in the PH_2 region.

Conclusion

$[CpRu(PPh_3)_2]^+$, generated in situ by chloride removal from $[CpRu(PPh_3)_2Cl]$, is a suitable synthon for the preparation of dinuclear ruthenium complexes containing tetraphosphorus or tetraphosphorus trisulfide as bridging ligand. The dinuclear complexes $[\{CpRu(PPh_3)_2\}_2(\mu,\eta^{1:1}\text{-}P_4)][CF_3SO_3]_2$ and $[\{CpRu(PPh_3)_2\}_2(\mu,\eta^{1:1}\text{-}P_{apical}\text{-}P_{basal}\text{-}P_4S_3)][CF_3SO_3]_2$ were prepared and characterised by elemental analysis, IR and NMR spectroscopy and X-ray crystallography. The last-named technique allowed important metrical parameters for this class of compounds to be collected. Remarkably, double metallation of both the P_4 and P_4S_3 ligands does not result in significant deformations with respect to the geometries of the free ligands or, in the case of the tetraphosphorus derivative, from the geometry of the mononuclear compound $[CpRu(PPh_3)_2(\eta^1\text{-}P_4)]CF_3SO_3$.

Both compounds react with an excess of water to undergo complete hydrolysis of the P_4 and P_4S_3 cages. Among the hydrolysis products the intriguing complexes $[\{CpRu(PPh_3)_2\}_2(\mu,\eta^{1:1}\text{-}P_2H_4)][CF_3SO_3]_2$ and $[CpRu(PPh_3)_2\{\eta^1\text{-}PH_2(SH)\}]CF_3SO_3$ were isolated and characterised by physicochemical measurements and X-ray diffraction. The dinuclear species contains a diphosphane ligand end-on coordinated to the two metal moieties, while the mononuclear compound is a unique complex in which a molecule of the practically unknown thiophosphinous acid is P-coordinated to the $CpRu(PPh_3)_2$ unit. In summary, this work confirms the extraordinary ability of the Ru complex fragment to stabilise as ligands very unusual and even unprecedented neutral molecules that are devoid of stability as free molecules.

Studies are in progress to expand the reactivity of the $\mu,\eta^{1:1}\text{-}P_4$ and $\mu,\eta^{1:1}\text{-}P_4S_3$ ligands and to unravel the mechanisms of their hydrolytic cleavage.

Experimental Section

All reactions and manipulations were performed under an atmosphere of dry, oxygen-free argon. The solvents were purified according to standard procedures.[40] ^1H, ^{19}F and ^{31}P NMR spectra were run on Varian Gemini g300bb and Bruker Avance 400 DRX spectrometers, equipped with variable-temperature control units accurate to ±0.1 °C. ^{19}F and ^{31}P chemical shifts are relative to external $CFCl_3$ and 85% H_3PO_4, respectively. ^1H chemical shifts are relative to tetramethylsilane as external reference and were calibrated against the residual solvent proton resonance. Coupling constants of **2**, **4** and **8** were obtained from 1D $^{31}P\{^1H\}$, ^1H and $^1H\{^{31}P\}$ NMR spectra with the aid of computer simulation using the gNMR program.[41] The ^{1}H NOESY spectra of compound **8** were recorded in $CHCl_3$ solution placed in an Evan's NMR tube, the inner tube of which was filled with $CDCl_3$ to provide a lock signal. Sixteen scans of 2-k size were acquired with 512 increments using a Watergate sequence for the optimisation of solvent signal and mixing times of 500 and 200 ms. ^{19}F NMR spectra of all compounds yielded a singlet at −75.5 ppm for the triflate anion. Mass spectra were carried out with a GCMS Shimadzu QP8000. Nujol-mull infrared spectra were run on a Perkin–Elmer Spectrum BX FT-IR spectrometer with samples between NaCl discs. Microanalyses were carried out at the Microanalytical Laboratory of the Department of Chemistry of the University of Firenze. $[CpRu(PPh_3)_2Cl]$[42] (**1**) and $[CpRu(PPh_3)_2(\eta^1\text{-}P_4)]CF_3SO_3$[25] were prepared according to the literature methods. H_3PO_2 and H_3PO_3 aqueous solutions (Aldrich) and PH_2Ph (Strem Chem) were used as received. P_4S_3 was obtained from Fluka AG and was recrystallised from toluene prior to use.

$[\{CpRu(PPh_3)_2\}_2(\mu,\eta^{1:1}\text{-}P_4)][CF_3SO_3]_2\cdot 3\,CH_2Cl_2$ (2)

Method A: A suspension of $[CpRu(PPh_3)_2Cl]$ (1.670 g, 2.30 mmol) and $AgCF_3SO_3$ (0.596 g, 2.31 mmol) in a mixture of THF (120 mL) and CH_2Cl_2 (120 mL) was added to a solution of P_4 (0.150 g, 1.16 mmol) in THF (40 mL). The resulting slurry was stirred at room temperature for 2 h and filtered. The solvent was then removed under vacuum to afford an orange solid, which was washed with toluene (20 mL) and *n*-pentane (2×10 mL) and dried. The solid was recrystallised from CH_2Cl_2 and *n*-hexane. Yield: 1.90 g (80 %); ^{1}H NMR (400.13 MHz; $CDCl_3$, 21 °C): $\delta = 7.50$–6.80 (m, 60 H; C_6H_5), 5.31 (s, 6 H; CH_2Cl_2), 4.77 ppm (s, 10 H; C_5H_5); $^{31}P\{^1H\}$ NMR (161.89, $CDCl_3$, 21 °C) $A_2A'_2MM'Q_2$ spin system: $\delta = 38.34$ ($^2J(P_A,P_M) = {}^2J(P_{A'},P_{M'}) = 49.43$, $^3J(P_A,P_{M'}) = {}^3J(P_{A'},P_M) = -1.60$, $^3J(P_A,P_Q) = {}^3J(P_{A'},P_Q) = 3.50$ Hz, 4 P; P_A and $P_{A'}$), −286.01 ($^1J(P_M,P_{M'}) = 212.60$, $^1J(P_M,P_Q) = {}^1J(P_{M'},P_Q) = 156.37$ Hz, 2 P; P_M and $P_{M'}$), −470.49 ppm (2 P; P_Q); elemental analysis calcd (%) for $C_{87}H_{76}Cl_6F_6O_6P_8Ru_2S_2$ (2058.2): C 50.77, H 3.72, P 12.04; found: C 50.21, H 3.90, P 12.06.

Method B: A suspension of $[CpRu(PPh_3)_2Cl]$ (360 mg, 0.5 mmol) and $AgCF_3SO_3$ (128 mg, 0.5 mmol) in a mixture of THF (25 mL) and CH_2Cl_2 (30 mL) was stirred at room temperature for 2 h and filtered. The resulting solution was added to $[CpRu(PPh_3)_2(\eta^1\text{-}P_4)]CF_3SO_3$ (480 mg, 0.5 mmol) in THF (25 mL) and CH_2Cl_2 (30 mL). The solution was stirred for 3 h and dimetal compound **2** was obtained as described under method A.

$[\{CpRu(PPh_3)_2\}_2(\mu,\eta^{1:1}\text{-}P_{apical}\text{-}P_{basal}\text{-}P_4S_3)][CF_3SO_3]_2\cdot 0.5\,C_7H_8$ (3): A suspension of $[CpRu(PPh_3)_2Cl]$ (2.18 g, 3.00 mmol) and $AgCF_3SO_3$ (0.770 g, 3.0 mmol) in a mixture of THF (120 mL) and CH_2Cl_2 (120 mL) was added to a solution of P_4S_3 (0.330 g, 1.50 mmol) in toluene (30 mL); the resulting slurry was stirred for 30 h and filtered. A yellow solid was obtained by the same procedure as for the P_4 complex. The crude compound was recrystallised from CH_2Cl_2 and toluene. Yield: 2.190 g (75 %); ^{1}H NMR (400.13, $CDCl_3$, 25 °C): $\delta = 7.60$–6.80 (m, 62 H; C_6H_5), 5.15 (s, 5 H; C_5H_5), 4.89 (s, 5 H; C_5H_5), 2.34 ppm (s, 2 H; $C_6H_5CH_3$); $^{31}P\{^1H\}$ NMR (161.89, $CDCl_3$, 25 °C): $\delta = 142.51$ (dtt, $^2J(P_F,P_M) = 25.00$, $^2J(P_F,P_B) = 40.03$, $^2J(P_F,P_Q) = 46.52$ Hz, 1 P; P_F), 38.54 (d, $^2J(P_A,P_M) = 39.12$ Hz, 2 P; P_A), 36.42 (d, 2 P; P_B), 2.13 (dtt, $^1J(P_M,P_Q) = 216.50$ Hz, 1 P; P_M), −129.07 ppm (dd, 2 P; P_Q); elemental analysis calcd (%) for $C_{87.5}H_{74}F_6O_6P_8Ru_2S_5$ (1945.7): C 54.01, H 3.83, P 12.73; found: C 53.94, H 3.90, P 12.67.

Hydrolysis of 2: Complex **2** (1.00 g, 0.49 mmol) was dissolved in THF (100 mL), H_2O (0.885 g, 49 mmol) was added and the resulting solution was stirred in a closed system at room temperature for 6 h; the red colour of the solution changed to orange. Mass spectra of the gas phase did not show hydrolysis products. The solvent was then removed under reduced pressure to yield an orange solid which, after extraction with H_2O (2×4 mL), was dried. ^1H-decoupled and ^1H-coupled ^{31}P NMR spectra of the aqueous solution showed resonances that were identical to those of pure H_3PO_2 and H_3PO_3 in the same solvent. The remaining solid was dissolved in acetone (10 mL), and diethyl ether (6 mL) was added; the resulting solution deposited overnight crude $[\{CpRu(PPh_3)_2\}_2(\mu,\eta^{1:1}\text{-}P_2H_4)][CF_3SO_3]_2$ (**4**) as a yellow solid, which was collected and dried. Evaporation of the solvent from the remaining solution left an orange solid the $^{31}P\{^1H\}$ NMR spectrum of which in $CDCl_3$ exhibited many resonances, among which those due to the cations $[CpRu(PPh_3)_2\{PH(OH)_2\}]^+$ (**5**), $[CpRu(PPh_3)_2\{P(OH)_3\}]^+$ (**6**) and $[CpRu(PPh_3)_2(PH_3)]^+$ (**7**) were identified.

$[\{CpRu(PPh_3)_2\}_2(\mu,\eta^{1:1}\text{-}P_2H_4)][CF_3SO_3]_2$ (4): The crude product, obtained as described above, was recrystallised from acetone and diethyl ether. Yield: 110 mg (13 %); ^{1}H NMR (400.13, $CDCl_3$, 21 °C): $\delta = 7.50$–6.80 (m, 60 H; C_6H_5), 4.88 (br d, $^1J(H,P_M) = {}^1J(H,P_{M'}) = 347.65$ Hz, 4 H; H_4P_2), 4.81 ppm (s, 10 H; C_5H_5); ^{31}P NMR (161.89, $CDCl_3$, 21 °C), $A_2A'_2MM'$ spin system: $\delta = 40.80$ ($^2J(P_A,P_M) = {}^2J(P_{A'},P_{M'}) = 43.08$, $^3J(P_A,P_{M'}) = {}^3J(P_{A'},P_M) = -6.52$, $^5J(P_A,P_{A'}) = 1.21$ Hz, 4 P; P_A and $P_{A'}$), −64.93 ppm ($J(P_M,P_{M'}) = 74.23$ Hz, 2 P; P_M and $P_{M'}$); IR (NaCl): $\tilde{\nu}(P{-}H) = 2320\ cm^{-1}$ (w); elemental analysis: calcd (%) for $C_{84}H_{74}F_6O_6P_6Ru_2S_2$ (1745.5): C 57.80, H 4.27, P 10.65; found: C 57.74, H 4.30, P 10.45.

Hydrolysis of 3: Complex **3** (1.00 g, 0.50 mmol) was dissolved in THF (100 mL), H_2O (0.900 g, 0.050 mmol) was added and the resulting was solution stirred at room temperature in a closed system for 2 h. The hydrolysis yielded gaseous species, which were partly absorbed in $CDCl_3$ or $(CD_3)_2CO$. The absence of any detectable signal in the $^{31}P\{^1H\}$ NMR spectra of these solutions ruled out the presence of phosphorus compounds in the gas phase, which, as revealed by gas mass measurements, contained only H_2S. Then, argon was bubbled through the solution and the vent gas was absorbed in aqueous copper(II) sulfate solution to yield a copious precipitate of copper sulfide. Once the H_2S was eliminated, the solvent was removed at reduced pressure to yield a yellow solid. ^{31}P NMR spectra of this solid dissolved in $CDCl_3$ showed the presence of hypophosphorous and phosphorous acids and the complex cations $[CpRu(PPh_3)_2\{PH(OH)_2\}]^+$ (**5**), $[CpRu(PPh_3)_2\{P(OH)_3\}]^+$ (**6**) and $[CpRu(PPh_3)_2(\eta^1\text{-}PH_2SH)]^+$ (**8**). Crude $[CpRu(PPh_3)_2(\eta^1\text{-}PH_2SH)]CF_3SO_3$ was obtained upon dissolving the mixture in acetone (6 mL) and removing half of the solvent under a slow stream of argon; the solid was collected by filtration and dried.

$[CpRu(PPh_3)_2(\eta^1\text{-}PH_2SH)]CF_3SO_3$ (8): The crude product, obtained as described above, was recrystallised from CH_2Cl_2 and *n*-hexane. Yield: 0.14 g (30 %); ^{1}H NMR (400.13, $CDCl_3$, 21 °C): $\delta = 7.54$–6.86 (m, 30 H; C_6H_6), 5.92 ($^2J(H_X,H_{X'}) = 18.21$, $^1J(H_X,P_M) = {}^1J(H_{X'},P_M) = 375.14$, $^3J(H_X,P_A) = {}^3J(H_{X'},P_{A'}) = 1.72$, $^3J(H_{X'},P_A) = {}^3J(H_X,P_{A'}) = 10.92$ Hz, 2 H; PH_2), 4.72 (s, 5 H; C_5H_5), 3.11 ppm (br, 1 H; SH); ^{31}P NMR (161.89; $CDCl_3$, 21 °C): $\delta = 42.42$ (d, $^2J(P_A,P_M) = 48.79$ Hz, 2 P; P_A), −32.64 ppm (t, 1 P; P_M); IR (NaCl): $\tilde{\nu}(P{-}H, S{-}H) = 2343\ cm^{-1}$; elemental analysis: calcd for $C_{42}H_{38}F_3O_3P_3RuS_2$: (905.8) C 55.69, H 4.23, P 10.25; found: C 55.57, H 4.30, P 10.14.

$[CpRu(PPh_3)_2(PH_2Ph)]CF_3SO_3$ (9): A suspension of $[CpRu(PPh_3)_2Cl]$ (360 mg, 0.5 mmol) and $AgCF_3SO_3$ (128 mg, 0.5 mmol) in a mixture of THF (25 mL) and CH_2Cl_2 (30 mL) was stirred at room temperature for 2 h and filtered. Neat PH_2Ph (55 mg, 0.5 mmol) was added to the filtered solution, and the system was stirred for 2 h. An orange solid was obtained upon removing the solvent under reduced pressure. The solid was recrystallised from CH_2Cl_2 and *n*-hexane. Yield: 380 mg (80 %); ^{1}H NMR (400.13, $CDCl_3$, 21 °C): $\delta = 7.50$–6.80 (m, 35 H; C_6H_5), 5.74 (dt, $^1J(H,P) = 357.60$, $^3J(H,P) = 6.93$ Hz, 2 H; H_2P), 4.59 ppm (s, 5 H; C_5H_5); ^{31}P NMR (161.89; $CDCl_3$, 21 °C), A_2M spin system: $\delta = 42.07$ (d, $^2J(P_A,P_M) = 40.30$ Hz, 2 P; P_A), −27.39 ppm (t, 1 P; P_M); IR (NaCl): $\tilde{\nu}(P{-}H) = 2334\ cm^{-1}$ (w); elemental analysis calcd (%) for $C_{48}H_{42}F_3O_3P_6RuS$ (949.9): C 60.69, H 4.46, P 9.78; found: C 60.71, H 4.51, P 9.64.

Crystallographic data collection and refinement procedures: Diffraction data for **2** at 293(2) K (with detector moved to 80 mm, due to long *b* axis), **4** at 170(2) K and **8** at 150(2) K were collected on an Oxford Diffraction Xcalibur 3 CCD diffractometer equipped with an Oxford Cryosystems apparatus, by using $Mo_{K\alpha}$ radiation ($\lambda = 0.71069$ Å). Data for **3**, in view of the small size of the crystal, were collected at 100(2) K by using $Cu_{K\alpha}$ radiation ($\lambda = 1.5418$ Å) on an Oxford Diffraction Xcalibur 3 CCD diffractometer, equipped with Oxford Cryosystems apparatus. Lattice constants were determined from the setting angles of 12532 reflections at $\theta = 3$–19° for **2**, 7681 at $\theta = 3$–17° for **3**, 3085 at $\theta = 3$–16 for **4** and 3387 at 3–14° for **8**. Intensity data were corrected for absorption effects by multiscan procedures using Oxford Diffraction software[43] (**2**, **3** and **8**) or SADABS[44] (**4**). Details of crystal data and refinement parameters are reported in Table 5. The structures were determined by direct methods with SIR97;[45] they were completed by difference Fourier proce-

Table 5. Selected crystallographic data for **2**·3 CH_2Cl_2, **3**·C_7H_8, **4** and **8**.

	2·3 CH_2Cl_2	**3**·C_7H_8	**4**	**8**
formula	$C_{87}H_{76}Cl_6F_6O_6P_8Ru_2S_2$	$C_{87.5}H_{74}F_6O_6P_8Ru_2S_5$	$C_{84}H_{74}F_6O_6P_6Ru_2S_2$	$C_{42}H_{38}F_3O_3P_3RuS_2$
M_r [g mol^{-1}]	2058.20	1945.67	1745.52	905.82
crystal size [mm]	0.24 × 0.30 × 0.30	0.06 × 0.10 × 0.15	0.20 × 0.25 × 0.40	0.05 × 0.25 × 0.50
$F(000)$	4168	3956	1780	1848
crystal system	monoclinic	monoclinic	triclinic	monoclinic
space group	$P2_1/c$	$P2_1/c$	$P\bar{1}$	$P2_1/c$
a [Å]	14.394(1)	14.3632(5)	11.140(2)	13.059(1)
b [Å]	44.569(2)	22.7195(7)	12.815(3)	14.868(2)
c [Å]	15.081(1)	26.1001(8)	15.328(3)	20.685(2)
α [°]	90	90	102.00(2)	90
β [°]	114.11(1)	96.272(3)	103.09(2)	104.83(1)
γ [°]	90	90	107.54(2)	90
V [Å^3]	8830.8(9)	8466.1(5)	1940.3(7)	3882.6(7)
Z	4	4	1	4
ρ_{calcd} [g cm^{-3}]	1.548	1.526	1.494	1.550
μ [mm^{-1}]	0.781	6.030	0.635	0.690
2θ range [°]	7.4–52.8	7.8–117.8	7.5–51.3	7.8–50.0
min/max transmission	0.868/1.140	0.712/1.261	0.784/1.000	0.915/1.095
measured reflections	155750	61389	15981	33858
independent reflections (R_{int})	17970 (0.061)	12047 (0.037)	6990 (0.030)	6849 (0.049)
observed reflections[a]	12421	8452	4863	4500
R_1/wR_2[b]	0.0869/0.1796	0.0680/0.1464	0.0653/0.0935	0.0589/0.0814
R_1/wR_2[a]	0.0625/0.1712	0.0471/0.1398	0.0392/0.0873	0.0357/0.0780
parameters/restraints	1066/20	1053/60	485/2	496
GoF	1.031	1.017	0.960	0.900
max/min $\Delta\delta$	1.895/−1.133	1.471/−0.614	1.049/−0.582	0.967/−0.343

[a] $F_o \geq 4.0\sigma(F_o)$. [b] All data.

dures and refined on F^2 by full-matrix least-squares methods.[46] Compound **2** crystallises with three dichloromethane molecules of solvation in the asymmetric unit, one of which was found to be affected by twofold orientational disorder. This was accounted for in the refinement, in which geometrical restraints were imposed on all C−Cl bond lengths, as well as on the C−C distances of two phenyl rings. Compound **3** crystallises as a toluene solvate with the toluene molecule disorderly arranged around an inversion centre (hence the hemisolvate formula). A few geometrical restraints were applied to part of a triflate anion. In the final refinement cycles of all structures the non-hydrogen atoms were refined anisotropically and hydrogen atoms were in geometrically generated positions, riding, except for the H atoms of the P_2H_4 moiety in **4** and the PH_2SH hydrogen atoms of **8**, the positions of which were allowed to refine (with a geometrical restraint for **4**). The isotropic displacement parameters of the hydrogen atoms were linked to the isotropic equivalent thermal parameters of the respective carrier atoms. Graphics were drawn with ORTEP.[47]

CCDC 631399 (**2**), 631400 (**3**), 631401 (**4**) and 631402 (**8**) contain the supplementary crystallographic data for this paper. These data can be obtained free of charge from the Cambridge Crystallographic Data Centre via www.ccdc.cam.ac.uk/data_request/cif.

Acknowledgements

Financial support by the Italian Ministero dell'Istruzione, dell'Università e della Ricerca is gratefully acknowledged.

---

[1] K. H. Whitmire, *Adv. Organomet. Chem.* **1998**, *42*, 1–145.
[2] O. J. Scherer, *Acc. Chem. Res.* **1999**, *32*, 751–762.
[3] M. Peruzzini, I. de los Rios, A. Romerosa, F. Vizza, *Eur. J. Inorg. Chem.* **2001**, 593–608.
[4] M. P. Ehses, A. Romerosa, M. Peruzzini, *Top. Curr. Chem.* **2002**, *220*, 107–140.
[5] M. Di Vaira, P. Stoppioni, M. Peruzzini, *Comments Inorg. Chem.* **1990**, *11*, 1–19.
[6] M. Di Vaira, P. Stoppioni, *Coord. Chem. Rev.* **1992**, *120*, 259–279.
[7] J. Wachter, *Angew. Chem.* **1998**, *110*, 782–800; *Angew. Chem. Int. Ed.* **1998**, *37*, 750–768.
[8] L. Y. Goh, *Coord. Chem. Rev.* **1999**, *37*, 751–768.
[9] M. Peruzzini, L. Gonsalvi, A. Romerosa, *Chem. Soc. Rev.* **2005**, *34*, 1038–1047.
[10] E. Urnèžius, W. W. Brennessel, C. J. Cramer, J. E. Ellis, P. von R. Schleyer, *Science* **2002**, *295*, 832–834, and references therein.
[11] J. Bai, A. V. Virovets, M. Scheer, *Angew. Chem.* **2002**, *114*, 1814–1817; *Angew. Chem. Int. Ed.* **2002**, *41*, 1737–1740.
[12] J. Bai, E. Leiner, M. Scheer, *Angew. Chem.* **2002**, *114*, 820–823; *Angew. Chem. Int. Ed.* **2002**, *41*, 783–786.
[13] J. Bai, A. V. Virovets, M. Scheer, *Science* **2003**, *300*, 781–783.
[14] P. Dapporto, S. Midollini, L. Sacconi, *Angew. Chem.* **1979**, *91*, 510; *Angew. Chem. Int. Ed. Engl.* **1979**, *18*, 469.
[15] P. Dapporto, L. Sacconi, P. Stoppioni, F. Zanobini, *Inorg. Chem.* **1981**, *20*, 3834–3839.
[16] M. Di Vaira, M. P. Ehses, M. Peruzzini, P. Stoppioni, *Eur. J. Inorg. Chem.* **2000**, 2193–2198.
[17] T. Gröer, G. Baum, M. Scheer, *Organometallics* **1998**, *17*, 5916–5919.
[18] A. W. Cordes, R. D. Joiner, E. D. Shores, *Inorg. Chem.* **1974**, *13*, 132–134.
[19] R. Jefferson, H. F. Klein, J. F. Nixon, *Chem. Commun.* **1969**, 536–537.
[20] M. Di Vaira, M. Peruzzini, P. Stoppioni, *Inorg. Chem.* **1983**, *22*, 2196–2198.
[21] M. Di Vaira, M. Peruzzini, P. Stoppioni, *J. Organomet. Chem.* **1983**, *258*, 373–381.
[22] E. Guidoboni, I. de los Rios, A. Ienco, L. Marvelli, C. Mealli, A. Romerosa, R. Rossi, M. Peruzzini, *Inorg. Chem.* **2002**, *41*, 659–668.
[23] I. de los Rios, J.-R. Hamon, P. Hamon, C. Lapinte, L. Toupet, A. Romerosa, M. Peruzzini, *Angew. Chem.* **2001**, *113*, 4028–4030; *Angew. Chem. Int. Ed.* **2001**, *40*, 3910–3912.

[24] F. H. Stephens, M. J. A. Johnson, C. C. Cummins, O. P. Kryatova, S. V. Kryatov, E. V. Rybak-Akimova, J. E. McDonough, C. D. Hoff, *J. Am. Chem. Soc.* **2005**, *127*, 15191–15200.

[25] M. Di Vaira, P. Frediani, S. Seniori Costantini, M. Peruzzini, P. Stoppioni, *Dalton Trans.* **2005**, 2234–2236.

[26] M. Peruzzini, M. Marvelli, A. Romerosa, R. Rossi, F. Vizza, F. Zanobini, *Eur. J. Inorg. Chem.* **1999**, 931–933.

[27] M. Di Vaira, I. de los Rios, F. Mani, M. Peruzzini, P. Stoppioni, *Eur. J. Inorg. Chem.* **2004**, 293–300.

[28] A. Adolf, M. Gonsior, I. Krossing, *J. Am. Chem. Soc.* **2002**, *124*, 7111–7116.

[29] M. Di Vaira, S. Seniori Costantini, F. Mani, M. Peruzzini, P. Stoppioni, *J. Organomet. Chem.* **2004**, *689*, 1757–1762.

[30] D. N. Akbayeva, M. Di Vaira, S. Seniori Costantini, M. Peruzzini, P. Stoppioni, *Dalton Trans.* **2006**, 389–395.

[31] A. M. Caminade, J. P. Majoral, R. Mathieu, *Chem. Rev.* **1991**, *91*, 575–612.

[32] C. G. Barlow, E. A. V. Ebsworth, G. C. Holywell, *Angew. Chem.* **1969**, *81*, 330; *Angew. Chem. Int. Ed. Engl.* **1969**, *8*, 372.

[33] D. Sellmann, *Angew. Chem.* **1973**, *85*, 1123; *Angew. Chem. Int. Ed. Engl.* **1973**, *12*, 1020–1021.

[34] M. Baudler, K. Glinka, *Chem. Rev.* **1994**, *94*, 1273–1297.

[35] W.-P. Meier, J. Strahle, E. Lindner, *Z. Anorg. Allg. Chem.* **1976**, *427*, 154–160.

[36] G. Balázs, J. C. Green, M. Scheer, *Chem. Eur. J.* **2006**, *12*, 8603–8608.

[37] P. W. Schenk, B. Leutner, *Angew. Chem.* **1966**, *78*, 942; *Angew. Chem. Int. Ed. Engl.* **1966**, *5*, 898.

[38] Z. Mielke, L. Andrews, *J. Phys. Chem.* **1993**, *97*, 4313–4319.

[39] W. N. Wang, W. L. Wang, Q. Luo, Q. S. Li, *Chem. Phys. Lett.* **2005**, *415*, 370–374, and reference therein.

[40] D. D. Perrin, W. L. F. Armarego, *Purification of Laboratory Chemicals*, 3rd ed., Pergamon, New York, **1988**.

[41] P. H. M. Budzelaar, gNMR V4.0, published by Cherwell Scientific Publishing, Copyright Iviry soft **1995–1997**.

[42] M. I. Bruce, C. Hameister, A. G. Swincer, R. C. Wallis, *Inorg. Synth.* **1990**, *28*, 270–272.

[43] Oxford Diffraction, CrysAlis CCD (Version 1.171.29.2), Oxford Diffraction Ltd, Abingdon (England), **2006**.

[44] G. M. Sheldrick, SADABS, Program for Empirical Absorption Corrections, University of Göttingen, Göttingen (Germany), **1986**.

[45] A. Altomare, M. C. Burla, M. Camalli, G. Cascarano, C. Giacovazzo, A. Guagliardi, A. G. Moliterni, G. Polidori, R. Spagna, *J. Appl. Crystallogr.* **1999**, *32*, 115–119.

[46] G. M. Sheldrick, SHELXL97, Program for Crystal Structure Refinement, University of Göttingen, Göttingen (Germany), **1986**.

[47] L. J. Farrugia, *J. Appl. Crystallogr.* **1997**, *30*, 565.

Received: December 21, 2006